

**Marine Mammal Monitoring on Navy Ranges (M3R)  
Passive Acoustic Monitoring of Abundance on the Pacific Missile Range  
Facility (PMRF) and the Southern California Offshore Anti-Submarine  
Warfare Range (SOAR)**

**3 March 2017**

**David Moretti  
Naval Undersea Warfare Center (NUWC), Newport, RI**

**Suggested Citation:**

**Moretti, D. 2017. Marine Mammal Monitoring on Navy Ranges (M3R) Passive Acoustic Monitoring of Abundance on the Pacific Missile Range Facility (PMRF) and the Southern California Offshore Anti-submarine Range (SOAR). Department of the Navy, Naval Undersea Warfare Center, Newport, RI. 3 March 2017.**

<b>REPORT DOCUMENTATION PAGE</b>		<i>Form Approved</i> <b>OMB No. 0704-0188</b>
Public reporting burden for this collection of information is estimated to average 1 hour per response, including the time for reviewing instructions, searching data sources, gathering and maintaining the data needed, and completing and reviewing the collection of information. Send comments regarding this burden estimate or any other aspect of this collection of information, including suggestions for reducing this burden to Washington Headquarters Service, Directorate for Information Operations and Reports, 1215 Jefferson Davis Highway, Suite 1204, Arlington, VA 22202-4302, and to the Office of Management and Budget, Paperwork Reduction Project (0704-0188) Washington, DC 20503. <b>PLEASE DO NOT RETURN YOUR FORM TO THE ABOVE ADDRESS.</b>		
<b>1. REPORT DATE</b> (DD-MM-YYYY) 03-03-2017	<b>2. REPORT TYPE</b> Monitoring report	<b>3. DATES COVERED</b> (From - To) 1 October 2015 - 30 September 2016
<b>4. TITLE AND SUBTITLE</b> MARINE MAMMAL MONITORING ON NAVY RANGES (M3R) PASSIVE ACOUSTIC MONITORING OF ABUNDANCE ON THE PACIFIC MISSILE RANGE FACILITY (PMRF) AND THE SOUTHERN CALIFORNIA OFFSHORE ANTI-SUBMARINE WARFARE RANGE (SOAR)	<b>5a. CONTRACT NUMBER</b>	
	<b>5b. GRANT NUMBER</b>	
	<b>5c. PROGRAM ELEMENT NUMBER</b>	
	<b>5d. PROJECT NUMBER</b>	
<b>6. AUTHOR(S)</b> David Moretti	<b>5e. TASK NUMBER</b>	
	<b>5f. WORK UNIT NUMBER</b>	
	<b>7. PERFORMING ORGANIZATION NAME(S) AND ADDRESS(ES)</b> Naval Undersea Warfare Center, Newport, RI	
<b>8. PERFORMING ORGANIZATION REPORT NUMBER</b>		
<b>9. SPONSORING/MONITORING AGENCY NAME(S) AND ADDRESS(ES)</b> Commander, U.S.Pacific Fleet, 250 Makalapa Dr. Pearl Harbor, HI	<b>10. SPONSOR/MONITOR'S ACRONYM(S)</b>	
	<b>11. SPONSORING/MONITORING AGENCY REPORT NUMBER</b>	
<b>12. DISTRIBUTION AVAILABILITY STATEMENT</b> Approved for public release; distribution is unlimited		
<b>13. SUPPLEMENTARY NOTES</b>		
<b>14. ABSTRACT</b> In FY16, the following tasks were completed by Marine Mammal Monitoring on Navy Ranges (M3R) at the Pacific Missile Range Facility (PMRF) off the Hawaiian Island of Kauai and the Southern California Offshore Range (SCORE) in the San Nicolas Basin off San Clemente Island: 1. System updates were carried out for both SOAR and PMRF. The software builds were completed, updated, and test readiness reviews (TRRs) were carried out in Newport. The update was installed at PMFR in January and the update at SOAR is scheduled for the week of 5-10 March 2017. The I/A package is making its way through NAVSEA Echelon II and incorporates the new risk management framework (RMF). This is the first I/A package from Newport to include the new RMF. 2. The packet recorder interface and new disk handling utilities were completed. Sample rate decimation was implemented and is undergoing testing. In addition, an X3 compression library has been implemented and is undergoing test. Upon conclusion of successful test the library will be integrated into the packet recorder software. 3. An initial risk function for Cuvier's beaked whales ( <i>Ziphius cavirostris</i> ) using the method described for Blainville's beaked whales ( <i>Mesoplodon densirostris</i> ) at the Atlantic Undersea Test and Evaluation Center (AUTC) by Moretti et al. 2010 was completed (Jones, et al.) as a proof-of-concept. This was the first application of passive acoustics methods to the derivation of a Cuvier's beaked whale risk function. The Risk Function estimates the probability of foraging dive disturbance as a function of sonar root-mean-squared receive level (RLrms). This effort also investigated an alternate methodology for determining RLrms by using the voltage level at each hydrophone (which is automatically recorded) as a proxy for received level at the animal as opposed to estimating the RLrms based on a propagation model. This		

method is faster and does not require precise ship tracks. It is presently being validated with data from a calibrated source, which was deployed from the R/V Sally Ride in January 2017 at SCORE.

4. Detection statistics (Probability of Detection (PD) and False Alarms (FA)) for M3R's Auto-Grouper program were derived and correction factors were calculated from beaked whale detections at SOAR (DiMarzio and Jarvis, in preparation). This effort also validated archived data products using raw data and calculated a density estimate of Blainville's Beaked Whales.

5. At SCORE, yearly abundance estimates showed no decline in population over the 5-year period, 2010-2014.

6. Beaked whale detection archives from both SPAWAR and M3R algorithms were compared and baseline abundance at PMRF was determined. There is no indication in a change in the population trend line over the five year period.

7. Satellite tags were placed on both Cuvier's beaked whales and fin whales at SCORE and multiple species at PMRF the results of which are provide in reports from MarEcoTel and Cascadia Research Collective respectively..

**15. SUBJECT TERMS**  
 Monitoring, passive acoustic monitoring, marine mammals, beaked whales, abundance, Hawaii Range Complex, Southern California Range Complex, Pacific Missile Range Facility, Southern California Offshore Range, mid-frequency active sonar

<b>16. SECURITY CLASSIFICATION OF:</b>			<b>17. LIMITATION OF ABSTRACT</b> UU	<b>18. NUMBER OF PAGES</b> 34	<b>19a. NAME OF RESPONSIBLE PERSON</b> Department of the Navy
<b>a. REPORT</b> Unclassified	<b>b. ABSTRACT</b> Unclassified	<b>c. THIS PAGE</b> Unclassified			<b>19b. TELEPHONE NUMBER (Include area code)</b> 808-471-6391

## Contents

List of Tables .....	2
List of Figures .....	2
Acronyms .....	3
1. Executive Summary .....	5
2. Background .....	6
3. M3R System Status .....	6
3.1 System Hardware .....	6
3.2 Information Assurance (IA) Approval .....	7
4. Zc Risk Function .....	7
4.1 Methodology .....	7
4.2 Analysis .....	9
4.3 Results .....	12
5. Detection Statistics .....	15
5.1 Background .....	15
5.2 Datasets .....	16
5.3 Methodology .....	17
5.4 Visual Zc Sightings vs. CTP .....	18
5.5 Manual Review vs. AG .....	20
6. Long Term Abundance and Density .....	24
6.1 Background .....	24
6.2 Dive Counting Methodology .....	25
6.3 SOAR Abundance .....	25
6.3 PMRF Abundance .....	29
6.4 Comparison of M3R and SPAWAR Algorithms .....	30
Works Cited .....	33

## List of Tables

Table 1. Data from passing known signals into the M3R replica setup. ....	12
Table 2. 2010-present available archives.....	17
Table 3. Click-Trains Associated with Four Different Sightings. ....	19
Table 4. Zc Click-Train Detected Within a Given Time Category.....	20
Table 5. Corrected Comparison of Filtered AG1 Output .....	22
Table 6. Detection Statistics for Dive Start Data.....	23
Table 7. Correction Factors for the AG Dive Start Results. ....	24
Table 8. Auto-grouper detection statistics. ....	24
Table 9. Correction factors. ....	24
Table 10. Mean dive rate and group size estimates .....	29
Table 11. 2010 estimate of Md abundance on PMRF .....	29
Table 12. A comparison of PMRF Blainville’s beaked whale dive detections. ....	31
Table 13. PMRF Md density calculations.....	31

## List of Figures

Figure 1: Density curve for the peak magnitude for sonar detections from 2012. ....	8
Figure 2. Thresholded sonar detector output for 2014.....	9
Figure 3. Thresholded sonar detector output for 2015.....	10
Figure 4. Density of dive durations.....	13
Figure 5. GAM fit. ....	14
Figure 6. The probability of GVP disturbance by sonar received level.....	15
Figure 7. Rating of Clicks.....	21
Figure 8. Yearly abundance at SOAR.....	27
Figure 9. Corrected estimate of yearly abundance at SOAR.....	28
Figure 10. Corrected composite estimate of monthly abundance at SOAR .....	28
Figure 11. Abundance estimates for 2010 – 2014 at PMRF.....	30

## Acronyms

AUTEC	Atlantic Undersea Test and Evaluation Center
A/D	Analog to Digital
AG	Auto-Grouper
ASP	Acoustic Signal Processor
BSURE	Barking Sands Underwater Range Expansion
CTF	Cable Termination Facility
CTP	Click Train Processor
CW	Continuous Wave
DIACAP	Defense Information Assurance Certification and Accreditation
DSP	Digital Signal Processor
FA	False Alarm
FFT	Fast Fourier Transform
FN	False Negative
FP	False Positive
GAM	Generalized Additive Model
GVP	Group Vocal Period
Hz	Hertz
IA	Information Assurance
M3R	Marine Mammal Monitoring on Navy Ranges
<i>Md</i>	<i>Mesoplodon densirostris</i> , Blainville's beaked whale
<i>Me</i>	<i>Mesoplodon europaeus</i> , Gervais' beaked whale
MFAS	Mid-Frequency Active Sonar
NAVSEA	Naval Sea Systems Command
PCAD	Population Consequences of Acoustic Disturbance
PD	Probability of Detection
PMRF	Pacific Missile Range Facility
RL <sub>rms</sub>	Received Level root mean squared
RMF	Risk Management Framework
SES	Shore Electronics System
SOAR	Southern California Anti-submarine Warfare Range
SPAWAR	Space and Naval Warfare Systems Command
SVMJ	Jarvis Support Vector Machine classifier
TDOA	Time Difference of Arrival
TRR	Test Readiness Review
<i>Zc</i>	<i>Ziphius cavirostris</i> , Cuvier's beaked whale

*This page intentionally left blank.*

## 1. Executive Summary

In FY16, the following tasks were completed by Marine Mammal Monitoring on Navy Ranges (M3R) at the Pacific Missile Range Facility (PMRF) off the Hawaiian island of Kauai and the Southern California Anti-Submarine Warfare Range (SOAR) in the San Nicolas Basin off San Clemente Island:

1. System updates were carried out for both SOAR and PMRF and included baleen Space and Naval Warfare Systems Command (SPAWAR) detection algorithms. The software builds were completed, updated, and test readiness reviews (TRRs) were carried out in Newport. The update was installed at PMRF in January and the update at SOAR is scheduled for 14-17 April 2017. The Information Assurance (IA) package is making its way through Naval Sea Systems Command (NAVSEA) Echelon II that incorporates the new risk management framework (RMF). This is the first IA package from Naval Undersea Warfare Center (NUWC), Newport to include the new RMF.
2. The packet recorder interface and new disk handling utilities were completed. Sample rate decimation was implemented and is undergoing testing. In addition, an X3 compression library has been implemented and is also undergoing test. The sample rate decimation along with the compression will allow extended data recordings on a single disc (months *vs.* days). Upon conclusion of successful tests, the library will be integrated into the packet recorder software.
3. An initial risk function for Cuvier's beaked whales (*Ziphius cavirostris*, *Zc*) at SOAR using the method described for Blainville's beaked whales (*Mesoplodon densirostris*, *Md*) at the Atlantic Undersea Test and Evaluation Center (AUTECE) was completed as a proof-of-concept [1]. This was the first application of passive acoustics methods to the derivation of a *Zc* risk function. The risk function estimates the probability of foraging dive disturbance as a function of sonar root-mean-squared received level ( $RL_{rms}$ ). This effort also investigated an alternate methodology for determining  $RL_{rms}$  by using the voltage level at each hydrophone (which is automatically recorded) as a proxy for received level at the animal as opposed to estimating the  $RL_{rms}$  based on a propagation model. This method is faster and does not require precise ship tracks. It is presently being validated with data from a calibrated source, which was deployed from the R/V *Sally Ride* in January 2017 at SOAR.
4. Detection statistics (Probability of Detection (PD) and False Alarms (FA)) for M3R's Auto-Grouper program were derived and correction factors were calculated from beaked whale detections at SOAR [2].
5. Corrected abundance estimates at SOAR were completed for 2010-2015. They showed no decline over the 5-year period, 2010-2014.
6. Beaked whale detection archives from both Space and Naval Warfare Systems Command (SPAWAR) and M3R algorithms were compared and baseline abundance at PMRF was determined. There is no indication in a change in the abundance trend line over the five-year period.

7. Satellite tags were placed on both *Zc* and fin whales (*Balaenoptera physalus*) at SOAR and multiple species at PMRF. The results will be provided in separate reports from MarEcoTel and Cascadia Research Collective to Commander, Pacific Fleet (COMPACFLT).

## 2. Background

At PMRF and SOAR, software and hardware is designed to run the M3R system with minimal operator intervention. The system collects passive acoustic detection archives on a nearly continuous basis [3,4]. These archive files provide an electronic record of marine mammal and sonar acoustic activity. They also provide marine mammal localizations from multiple algorithms with a focus on *Md* and *Zc*. As new algorithms become available and are incorporated into the system, algorithm-specific reports can be seamlessly integrated into the archives to provide a time-synchronous history of events. Currently, both the Matsuyama/ Martin and the Helble baleen algorithms [5] are being integrated into the software build.

These acoustic and geographic data are used to the study of the effect of sonar on marine mammals. For example, prior and on-going studies have established that beaked whales are displaced when exposed to Mid-Frequency Active Sonar (MFAS) [6]. The research suggests they increase their time submerged and ascend to the surface away from the source [7, 8]. By combining passive acoustic localization of the animals and precise location of sonar sources, a risk function for behavioral disruption of *Md* at AUTECH was developed [9]. Cross-validating the risk function with *Md* data from PMRF is underway. The results from AUTECH have been used to develop an *Md* Population Consequences of Acoustic Disturbance (PCAD) model to estimate the cumulative effect of repeated sonar exposure on a population level, a key concern from an environmental management perspective [10]. In 2016, the PCAD is being adapted for use with *Zc* at SOAR.

## 3. M3R System Status

The transition of a prototype system with a set of user utilities and the installation of flash drives were completed at both PMRF and SOAR. The systems provide basic passive acoustic detection data to support passive acoustic species monitoring by on-site range personnel. The software builds were completed, updated, and TRRs were carried out in Newport. The update was recently completed at PMRF and the update at SOAR is scheduled for the week of 14-17 April 2017. The Information Assurance (IA) package is making its way through NAVSEA Echelon 2 and incorporates the new risk management framework. This is the first IA package from Newport to include the new framework.

### 3.1 System Hardware

SOAR was retrofitted with new drives and the network link replaced with A/D converters as part of the IA requirements. A new data collection node configured with three General Standards 64-channel analog to digital converters was installed along with a new patch panel, and 100 additional BNC cables were run from the Shore Electronics System (SES) analog outputs to the M3R signal processor. These modifications allowed removal of the network data link from the M3R signal processor to the SOAR acoustic signal processor (ASP) as mandated by the IA requirements.

All mechanical drives have now been replaced with flash drives at both SOAR and PMRF. This required modifications to the M3R software build. The new build was tested in Newport and a TRR was successfully completed. The removal of mechanical drives will provide increased system reliability in both the SOAR cable termination shelter (CTS) on San Clemente Island and in the Barking Sands Underwater Range Expansion (BSURE) room at PMRF where power outages are a significant issue. Also, the flash disks are mandated by the M3R IA package and will make the required patching possible. New software builds with the required patches will be produced in Newport. The systems will be updated through the delivery of new flash cards. As specified in the IA plan, software upgrades will occur twice per year.

### 3.2 Information Assurance (IA) Approval

Operation of all computer based hardware within Navy facilities requires Information Assurance (IA) approval. The architecture of all major range Digital Signal Processors (DSPs) evolved from the M3R signal processor architecture. In 2016 a new IA package was submitted under the new risk management framework (RMF) which replaced the Defense Information Assurance Certification and Accreditation (DIACAP) Process. The package has been accepted by NAVSEA (Echelon II). Both PMRF and SOAR are awaiting final approval.

## 4. Zc Risk Function

### 4.1 Methodology

In 2016, a preliminary behavioral risk function for  $Z_c$  was completed using the method described for  $M_d$  [9]. This risk function estimates the probability of foraging dive disruption as a function of MFAS  $RL_{rms}$ .

Data from SOAR during four time windows were analyzed: 3-10 Feb 2012; 27 January–22 March 2014; 15 April–29 May 2015; and 6– 8 October 2015.  $Z_c$  groups were extracted from time periods before and during MFAS operations. For times during MFAS transmissions the maximum exposure level for each dive was estimated. M3R then fit a generalized additive model (GAM) with a binomial response to predict the probability of a dive starting on each hydrophone as a function of the maximum  $RL_{rms}$  in a 30-minute period.

Sonar pings were detected in M3R data archives. Fast Fourier Transform (FFT)-based detection reports were examined. Three separate sonar detector configurations were used that included 2,500-4,400 Hertz (Hz); 3,300-4,900 Hz; and 6,500– 8,500 Hz frequency bands. The sonar detector required a minimum of 10 detections in-band within a 1-second window. Because the frequency bands overlap, it is possible that the same sonar ping could be simultaneously detected multiple times. However, the final analysis relied only on the peak detection magnitude across all frequency bands, so a single ping that was detected in multiple bands would only be counted once. In addition, we limited the sonar detector output to consist only of detection events with a peak magnitude greater than 0.66 volts to reduce the amount of false detections (Figure 1). This threshold was determined by assuming that the log transformed peak magnitude of noise observations was normally distributed and then including only observations at least three standard deviations above the mean of the estimated noise distribution. The resulting sonar

dataset consisted of the hydrophone ID, time, and maximum voltage for each detected ping and formed the first of two datasets in our analysis.

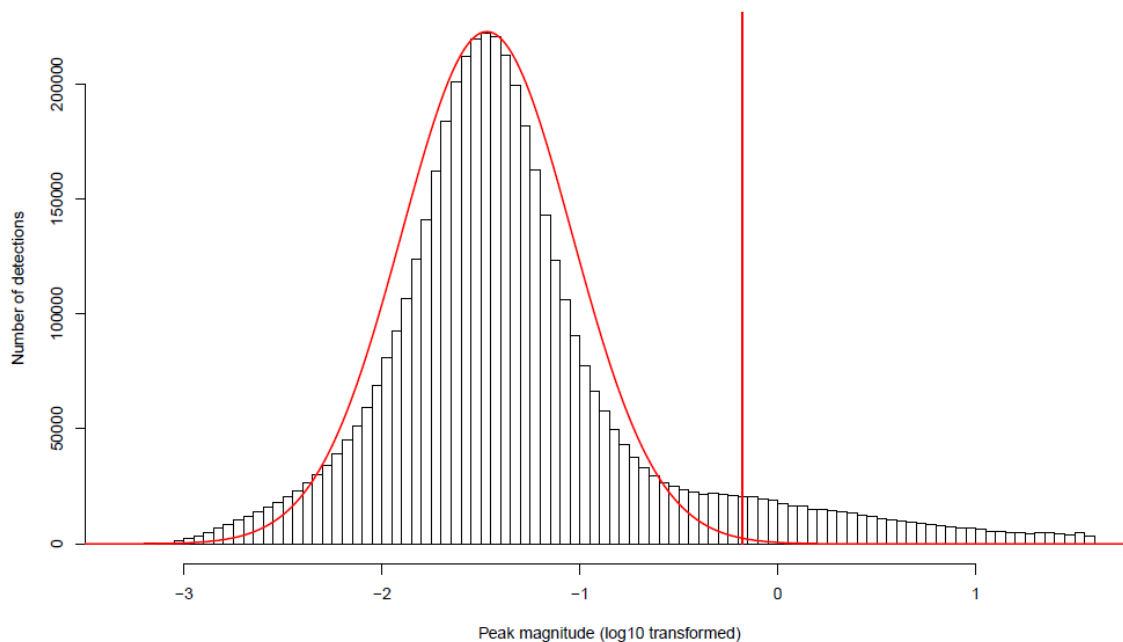


*Figure 1: The density curve for the peak magnitude for sonar detections from 2012 is plotted here. The height of each bar indicates the number of detections with a peak magnitude in the range indicated on the horizontal axis. The red curve depicts the density of a normal distribution whose parameters were estimated to approximate the observed data. The vertical red line indicates the threshold used to identify sonar. The peak magnitude is a log transformation of the raw value reported by the sonar detector prior to voltage conversion.*

The second dataset contained a set of beaked whale detections. These detections were found by first identifying individual beaked whale clicks in the archived hydrophone data, then using a program called “Autogrouper” to cluster sets of clicks into group vocal periods (GVPs). The program grouped individual clicks into click trains and associated click trains across hydrophones. The output of this algorithm was a list of records that included the ID number of the hydrophone that detected each GVP, the number of detected clicks, and the start and end times for each GVP. Only GVPs with a minimum of 500 clicks were retained for the analysis. The group center hydrophone was assigned to the hydrophone with the greatest number of click detections. The whale detection process is described in greater detail in [2].

## 4.2 Analysis

The start of vocalizations in beaked whales is associated with the start of a foraging dive, so a lack of dive starts may indicate that foraging behavior has been disrupted [1, 11]. To estimate the risk function, first the probability of a dive start ahead of a sonar operation was estimated. Next, a GAM was used to predict the probability of a dive start as a function of the estimated  $RL_{rms}$  [9]. These data were then compared to estimate the probability of dive disruption as a function of  $RL_{rms}$ . The modeling approach is based on the methodology described in [9].

First, periods of sonar activity were identified based on the distribution of sonar detector output per unit time (Figures 2 & 3). An active sonar scenario was defined as each time period when the sonar detector identified a minimum of 200 hundred pings and was included in the analysis. In total, we identified 61 active sonar scenarios with a total duration of 270.5 hours, and a baseline scenario without sonar that lasted for 96 hours.

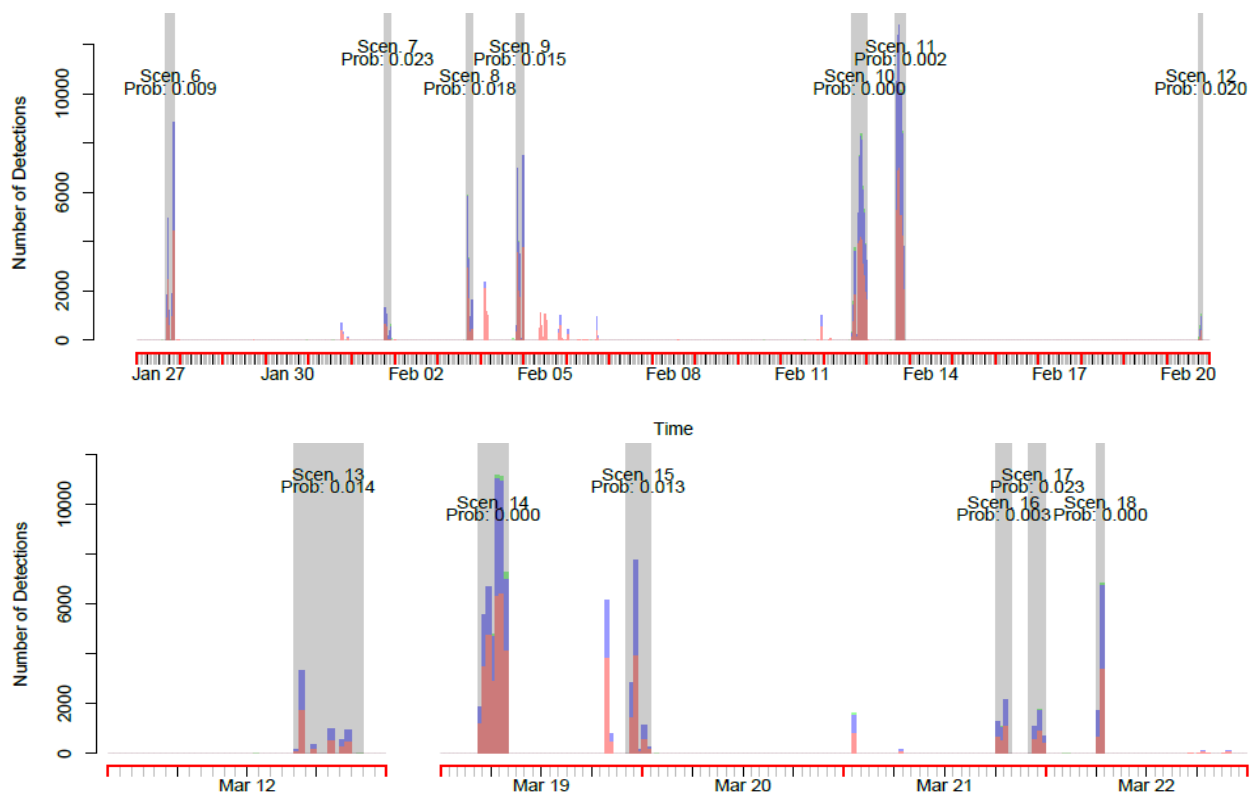


Figure 2. The thresholded sonar detector output is plotted for 2014 (top and bottom). The total height of each bar indicates the number of sonar detections that occurred during that 1/2 hour window, and the bars are colored according to the band within which the detections happened. Due to the overlap between the 2,500-4,400 Hz and 3,300-4,900 Hz bands, some sonar pings may be counted twice. The active sonar scenarios are highlighted in gray. Each scenario is identified by an id number and is also labeled with the proportion of hydrophone-time interval

pairs during which a GVP started as described by Equation 2. Red ticks on the horizontal axis indicate breaks in days, black indicate 6 hour intervals, and gray ticks are hourly. Note that time scales are different for top and bottom plots.

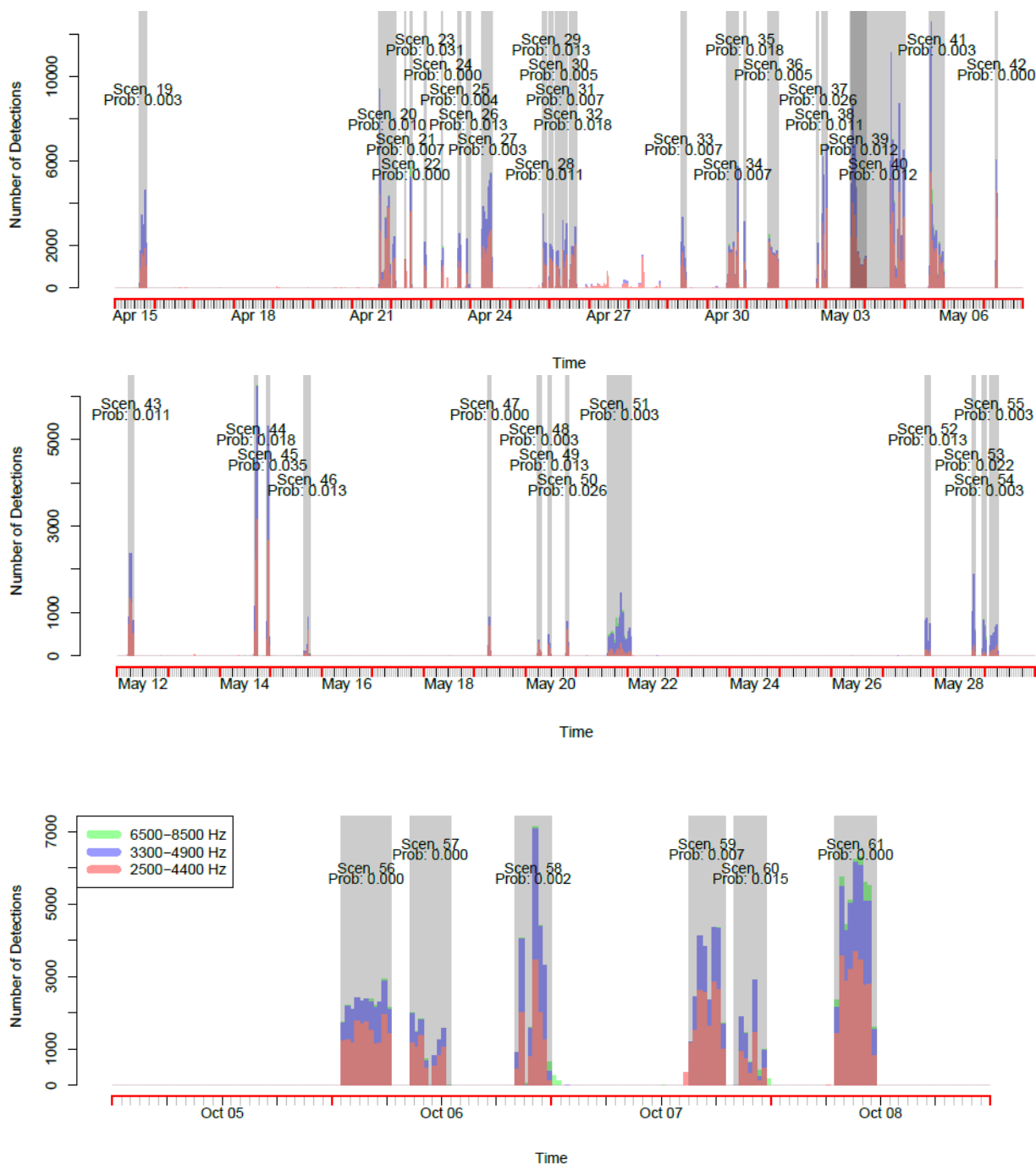


Figure 3. The thresholded sonar detector output is plotted for 2015. This figure is otherwise the same as Figure 2.

Data were binned into  $\frac{1}{2}$  hour time windows and the probability of a GVP starting within each 0.5-hour window was estimated. Let  $w_{ij}$  be an indicator variable that takes value 1 if hydrophone  $i$  was the central hydrophone for at least 1 GVP that started during time window  $j$  and 0 otherwise. For  $K$  hydrophones and  $T$  time windows, the GVP start probability was computed as (Equation 1):

$$\hat{P} = \sum_{i=1}^K \sum_{j=1}^T \frac{w_{ij}}{KT} \quad (1)$$

For the AUTECH analysis,  $RL_{rms}$  for each period was estimated via a propagation model. Here the maximum receive level of sonar on every hydrophone was measured for each 0.5-hour time window. The voltage for each hydrophone-time window was set to the greater of 0V, which was assumed to represent the ambient level or the maximum peak voltage across all sonar detections on that hydrophone within that time window. We refer to this dataset as the full sonar dataset, and also constructed a second dataset from this one. The second dataset, which we refer to as the reduced dataset, excludes hydrophone-time window pairs that did not include a sonar detection. This dataset removes the arbitrary assumption that 0 V represents the ambient noise level. The peak voltages in each dataset were mapped to received sound pressure levels by first estimating the voltage at the input to the M3R processing system from the recorded voltage, then by estimating the received pressure level at the hydrophone face from the M3R input voltage.

To calibrate the M3R voltage response, we input a 3,492 Hz continuous wave (CW) 1-second ping into the M3R signal processor analog to digital converter (A/D). The input peak-to-peak voltage varied from 18.2 to 0.648  $V_{p-p}$ . Detection archives were recorded and the peak voltage reported by the FFT detector for each ping was noted. A linear model was used to relate the input voltage to the output level reported by the detector. The measured data are presented in Table 1, and resulting equation is given by

$$V_{in} = 0.777739V_{out} + 0.066631 \quad (R=0.9996, p=1.2e-7) \quad (2)$$

The conversion from  $V_{in}$  to the received level (PL recv) was computed from the information reported in the BSURE Refurbishment Manual, Appendix B as  $PL_{recv} = 20 \log_{10} (\sqrt{0.5} V_{in}) + 122.34 \text{ dB re } 1 \mu\text{Pa}$ .

*Table 1. The observed data from passing known signals into the M3R replica setup are shown here. A 3492 Hz sine wave was passed through an attenuator, then into an oscilloscope and the replica M3R setup.*

Attenuation (dB)	SPC archive voltage (V)	Oscilloscope voltage (V <sub>p-p</sub> )
0	23.5	18.2
-6	11.9	9.6
-12	5.83	4.7
-18	3.00	2.27
-24	1.50	1.17
-29	0.80	0.648

We fit a GAM with a binomial response and logit link function to predict the probability of a dive starting on each hydrophone during each time period given each estimated  $RL_{rms}$ . Based upon visual inspection of the trial fits, we determined that a GAM with 3 knots was ideal.

### 4.3 Results

A GVP start occurred on 0.75% of the hydrophone-time window pairs during the active sonar scenarios, which is significantly different than the 3.0% from the baseline scenario (Pearson's  $\chi^2$ -test,  $\chi^2=409.41$ ,  $df=1$ ,  $p\leq 2.2e-16$ ). The GVPs varied in length, but were all less than 1 hour long (Figure 4). 39.5% of the hydrophone-time window pairs that occurred during the active sonar scenarios included a sonar detection, and 63.2% of the hydrophone-time window pairs with a GVP start also had a sonar detection. The difference in GVP start probabilities between hydrophone-time window pairs with and without sonar detections was significant (Pearson's  $\chi^2$ -test,  $\chi^2=71.72$ ,  $df=1$ ,  $p\leq 2.2e-16$ ).

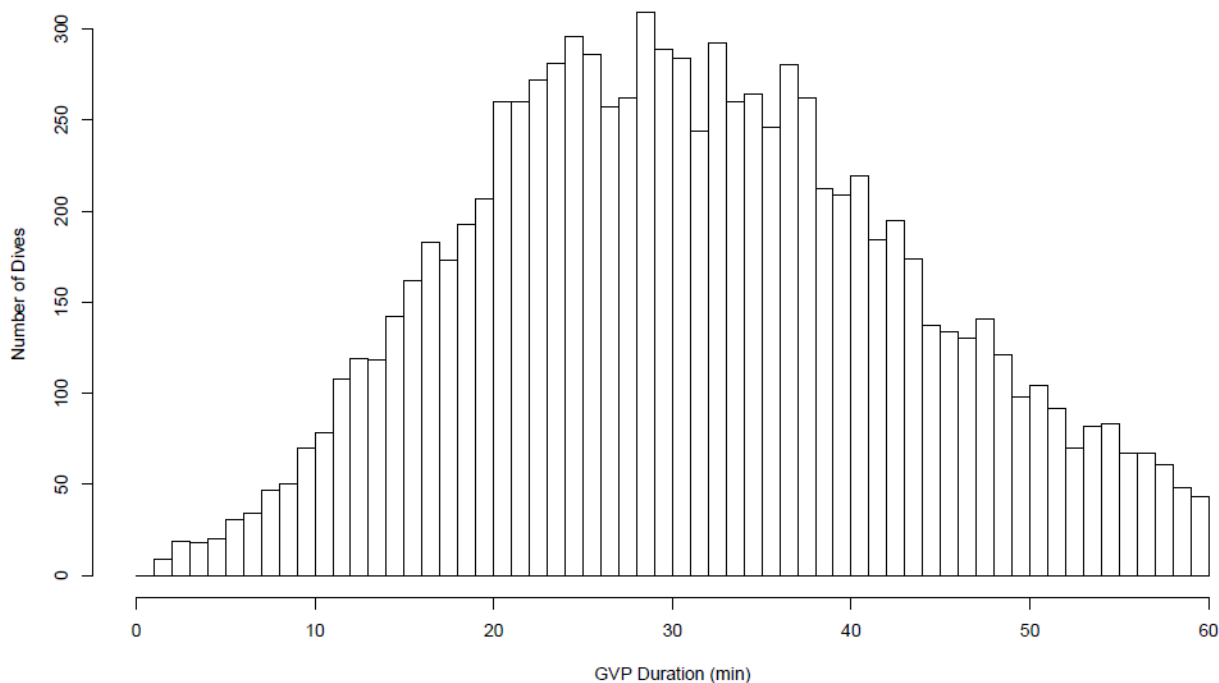


Figure 4. The density of dive durations is shown using a 1 minute bin size. Note that GVPs with duration of 60 minutes or greater are not included in the analysis.

The fitted GAM predicted that the highest probability of a GVP start occurs at moderate sonar intensity, particularly when fit to the full dataset (Figure 5). However, when the GAM was fit to the reduced dataset, the predicted GVP start probability at the lowest received sonar level was not significantly different from the highest predicted GVP start probability. Fitted probabilities at both high and low received levels were less than 0.5%, and the maximum fitted probability was 1.73%. All of the fitted probabilities during sonar exercises were significantly lower than the baseline probability of 3.0%.

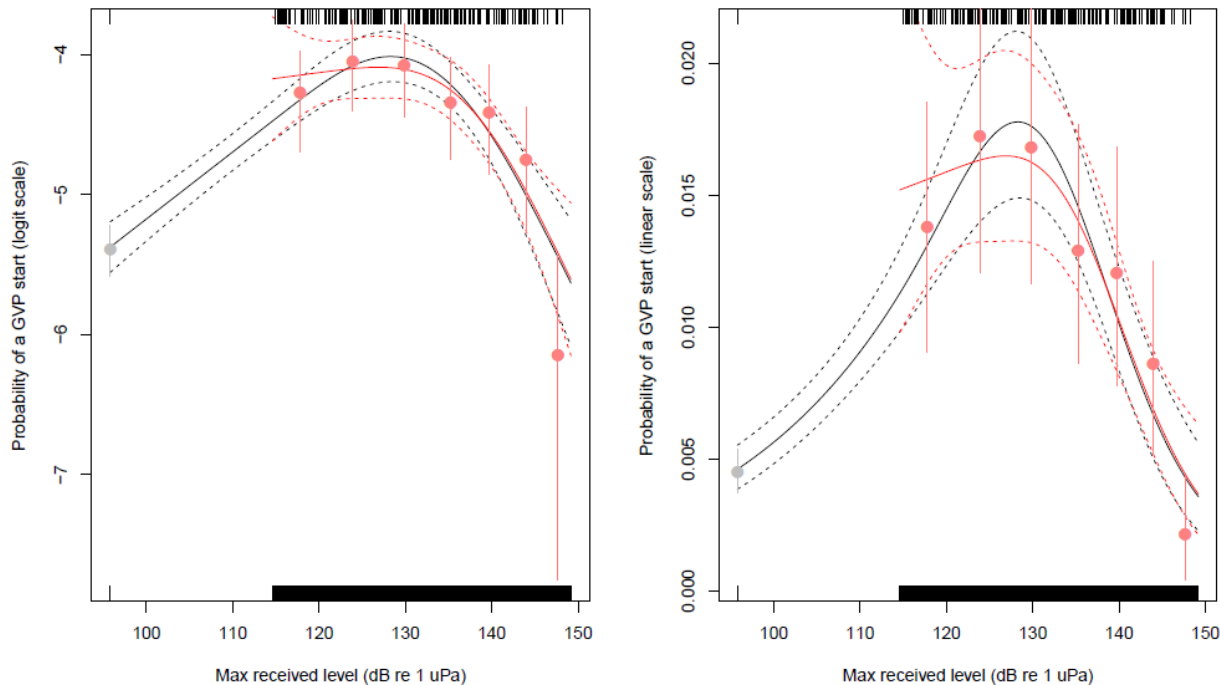


Figure 5. The GAM fit is depicted here on logit (left) and linear (right) vertical scales. The GAM fit is given by the solid line and a 95% confidence interval is given by the dashed lines. The first (gray) dot is an estimate for  $\hat{P}$  from the hydrophone-time window records without a sonar detection, and the other (red) dots give estimates from approximately 1/7th of the remaining data. The vertical bars through these dots indicate 95% binomial confidence intervals. The leftmost dot contains all of the hydrophone-time window pairs for which there was not a sonar detection. The rug plot at the bottom depicts the density of samples that did not include a GVP start, and the rug plot at the top depicts the samples for which there was a GVP start.

Overall, the probability of GVP disturbance was predicted to be lowest at moderate sonar intensity and highest at high sonar intensity (Figure 6). As with the GAM fits, the fit to the reduced dataset does not show a significant difference between the probability of disturbance at the lowest recorded sonar intensity and the lowest probability of disturbance, but does show a significant increase in the probability of disturbance at high sonar intensity. The probability of disturbance in the reduced fit ranged from 43.0% at moderate sonar intensity to 86.9% at high sonar intensity.

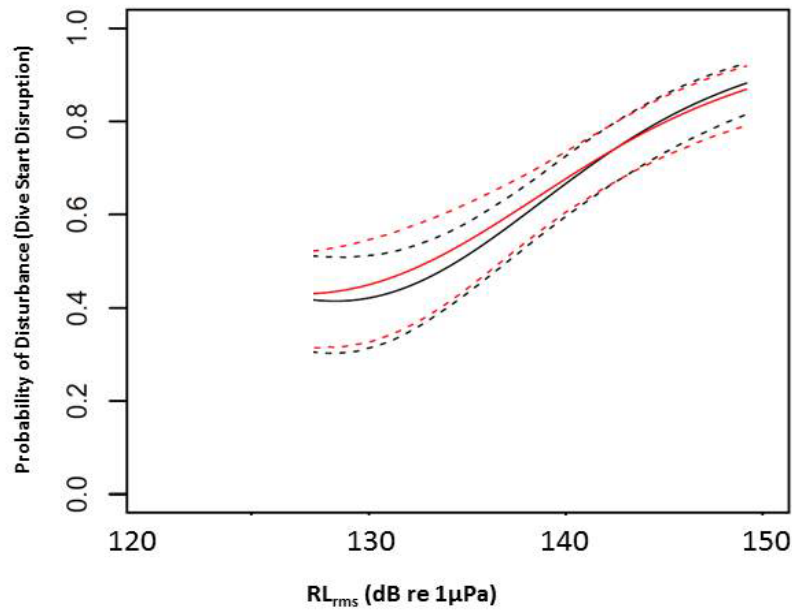


Figure 6. The probability of GVP disturbance by sonar received level is shown as estimated by fitting a GAM. The black curves show the result from the GAM fit to the full dataset (solid line) with a 95% confidence interval (dashed lines). The red curves show the same information for the GAM fit to the reduced dataset.

The results provide preliminary evidence that the sonar detector reports can be used to approximate the impact of active sonar on beaked whale behavior. As with *Md* at AUTEK, the number of foraging dive starts measured is reduced as a function of sonar received level. Given the preliminary analysis, these data can be used to inform the continued derivation of a  $Z_c$  behavioral risk function.

## 5. Detection Statistics

### 5.1 Background

The following section on Detection Statistics is extracted from a Technical Memo [2]. These statistics were calculated to help investigate  $Z_c$  temporal and spatial distribution, and develop a habitat model based on oceanographic factors, prey distribution, and sonar (MFAS) received level. Specifically, this effort developed the PD and FA for M3R's Auto-Grouper (AG). The AG automates the grouping process by evaluating the click-train output using a set of rules to determine which click-trains form a  $Z_c$  group. These factors are incorporated into methods for  $Z_c$  long-term abundance estimation.

## 5.2 Datasets

The M3R system uses the bottom-mounted hydrophones on the U.S. Navy test and training ranges to automatically detect, classify, and localize marine mammal vocalizations in real-time. M3R collects continuous, year-round archives of acoustic detections, calculates the time differences of arrival (TDOAs) and localizations from all range hydrophones, and periodically gathers raw acoustic recordings from all hydrophones on the range. These archive files include both marine mammal vocalizations and sonar, and can be replayed for later analysis [6, 12]. The acoustic detection archives were the primary source of data for this project.

The M3R class-specific support vector machine (CS-SVM) classifier algorithm provides robust real-time, automated detection and classification of six different categories of call types within four classes of animals [3]. Detection archives are available from all refurbished range hydrophones for most months of the year since May 2010 (Table 2). For this effort, 26,768.5 hours of archive data between August 23, 2010 and November 15, 2015 were catalogued and processed through the Click Train Processor (CTP), auto-grouper, and sonar detector in order to derive detection statistics and correction factors for the AG.

*Table 2. Days from 2010 to the Present for Which SOAR CS-SVM Detection Archive Files Are Available. CS-SVM Zc Foraging-Click Detections Are Available from May 10-16, 2010 (Blue), While CS-SVM Zc Buzz Click Detections Were First Recorded in July 17-29 and 31, 2014 (Pink).*

SOAR Detection Archives												
	Jan	Feb	Mar	Apr	May	Jun	Jul	Aug	Sep	Oct	Nov	Dec
2010					10-16			23-31	1-30	1-10, 13-31	1-6, 9-11, 18-30	1-14, 16, 23-30
2011	4-25	1-2, 4-28	1-8	5-7	19-31		26-31	1-25, 29-31	1-30	1-31	1-14, 23-30	1-31
2012	1-8, 10-26, 30-31	1-23	14-31	1-30	1-12, 14, 29-30	1-4, 7-8	31	1-3, 7		15-31	1-2, 14-24	8-17
2013					15-31	1-30	1-15, 23-31	1-31	1-30	1-4, 30-31	1-2	20-31
2014	1-31	1-13, 20-28	1-3, 7-31	1-2, 4-30	1-13, 17-31	1-17	17-29, 31	1-12, 27-31	1-2, 5-30	1-14	20, 28-30	1-31
2015	1-31	1-28	1-4, 10-21, 24-31	1, 7-30	1-31	1-2, 8-14, 24-27, 29-30	1, 8-28	11-31	1-15	2-31	1-15	21-31
2016	1-31	1-9, 12-29	1-31	1-20, 26-30	1-9, 23-31	1-6, 20-present						

### 5.3 Methodology

Two approaches were used to determine detection statistics. The first approach compared Zc click-trains to visually-verified sightings of Zc on the range. A temporal and spatial window around the start time and location of each visual sighting was examined for the presence of Zc click-trains. This approach had the advantage of comparing Zc click-train detections with a known presence of Zc; however, a false positive error rate for the detection process could not be determined with this method.

In the second approach, the Zc groups generated by the AG program were compared to a manual review of samples of the archive data using MMAMMAL. The Zc groups determined by manual review were considered 'truth,' and the PD, percent of false negatives (FN), percent of false positives (FP), and FN and FP correction factors were calculated for the AG program.

## 5.4 Visual *Zc* Sightings vs. CTP

In the first approach, the *Zc* click-trains generated by CTP were examined in a temporal and spatial window around the start time and location of *Zc* sightings on the SOAR range. MarEcoTel personnel provided data on their visual sightings conducted on the SOAR range between 2006 and 2015. From these, 32 visual sightings of *Zc* that had corresponding M3R archive files between 2011 and 2015 were extracted. The sighting data provided information including the date, species, time and location at the start of the sighting, the end time and location of the sighting (which corresponded to the time the sighting ended, and not necessarily when a *Zc* group went on a deep foraging dive), the number of animals in the group and their behavior.

In order to determine if the sighted animals were detected, archives corresponding to the time of the sighting were identified and run through CTP. The CTP outputs were then filtered for CS-SVM detections (detector type 17), *Zc* foraging click class (class 2), and ICI between 0.35 and 0.75 seconds. The mean and standard deviation of the remaining click-train click counts were calculated. Two cases were considered: 1) only click-trains with click counts either greater than or equal to the mean, and 2) only click trains with click counts greater than or equal to the mean plus one standard deviation.

The time window was based on the foraging dive cycle for *Zc* tagged on the SOAR range [13]. The group mean ( $\mu$ ) for the foraging dive cycle is 170.1 minutes, and the standard deviation ( $\sigma$ ) is 29.3 minutes (G. Schorr, personal communication). The foraging dive cycle was centered on the start of a sighting, and either the mean or the mean plus one standard deviation was used, resulting in a time window of either  $\pm 85$  minutes ( $\mu/2$ ) or 100 minutes ( $\mu/2 + \sigma/2$ ) before and after the sighting start time. The spatial window was based on the modelled detection distance for *Zc* at the surface [14] and the mean straight-line movement of *Zc* over the course of a sighting. The mean minimum straight-line speed was 1.38 km/hr. [15]. The maximum detection distance was modelled to be 4 km for *Zc*, although this was for a hydrophone near the surface, rather than for bottom-mounted hydrophones, such as those at SOAR [14]. Over the time windows stated above, this would translate to between 1.96 and 2.31 km before or after the sighting start. These distances were added, and a spatial window of radius 6.31 km was used, which was centered on the location at the start of the sighting and included all hydrophones included in this radius.

The hydrophones within the spatial window and those that included *Zc* click-trains within the time window were identified for each sighting. Filtered *Zc* click-trains that fell within the window were categorized as either occurring before the sighting start (yellow), after the sighting end (blue), overlapping the sighting period (pink: before/during, during, or during/after) or unknown (green), in cases in which there was no end time recorded. Examples of sightings associated with click-trains with total click counts greater than or equal to the click count mean are shown in Table 3.

Table 3. Example of the Click-Trains Associated with Four Different Sightings, for Click-Trains with Total Click Counts >  $\mu$  Click Count. Filtered Zc click-trains occurring before the sighting start are shown in yellow; after the sighting ended are shown in blue; overlapping the sighting period are in pink; and cases in which there was no end time recorded are shown in green.

Julian Day	UTC Start Time	Start Closest Hyd	UTC End Time	End Closest Hyd	Hyds within Range 6310m of Start Lat/Lon	Hyds Detected within Range 6310m	Hyd with Max # Clicks	Max # Clicks	Start Time Hyd Max # Clicks	End Time Hyd Max # Clicks	ICI
005	19:57	406	23:49	32	306,307,405,406,407,506	306,405	306	2025	18:18:02	18:52:51	0.547
006	17:24	607	18:45	40	506,606,607,708	506,606,607,708	607	1892	16:04:04	16:42:21	0.551
							607	2216	16:48:06	17:19:31	0.554
							506	2120	17:26:00	18:13:09	0.538
							607	2338	17:58:40	18:36:02	0.581
006	20:02	607	20:56	607	506,606,607,608,708,709	506,606,607,608,708,709	606	1185	19:44:44	20:17:35	0.537
							506	466	20:34:59	21:08:24	0.556
							608	2526	20:35:05	21:18:31	0.551
							606	443	21:21:03	21:39:01	0.522
011	20:23	309	N/A		408	408	308	388	19:38:23	20:00:24	0.468
							408	2409	19:53:56	20:27:55	0.537
							208	226	19:57:22	20:05:42	0.567
							308	786	20:03:34	20:23:55	0.549
							309	532	20:25:19	20:57:02	0.538
							308	275	20:27:25	20:41:02	0.555
							308	558	20:59:10	21:16:23	0.542

For every sighting, each click-train time category was then assigned a '1' or '0' depending on whether a click-train occurred in that category and the totals were summed. The total number of occurrences of each category was also tabulated and the values were summed (Table 4).

*Table 4. Total Number of Instances of a Zc Click-Train Being Detected Within a Given Time Category, Referenced to the Start of the Zc Sighting. Results for Click-Trains with Total Click Counts  $\geq \mu$  or  $\geq \mu + 1 \sigma$ .*

<b>Count Summary</b>	<b>Total # Sightings</b>	<b>Before</b>	<b>After</b>	<b>During</b>	<b>Before/During</b>	<b>During/After</b>	<b>Before/Unknown</b>	<b>Unknown (During/After)</b>
$\mu$	32	68	10	24	9	5	3	25
$\mu + 1 \text{ sd}$	32	33	6	12	5	4	0	12

The results show that for each visual sighting of *Zc*, click-trains are nearly always detected either before or after the sighting, within the time and spatial window that the group is expected to be on a deep foraging dive. If click-trains with click counts lower than the mean were added, more click-trains would be detected. However, quite often *Zc* click-trains were also detected while the group was on the surface. Since *Zc* only vocalize while on deep foraging dives, this indicates that either there were other *Zc* groups foraging in the vicinity, the group's diving behavior was more asynchronous than expected (i.e. some individuals were diving while others were on the surface), or that these click trains were false detections [11].

## 5.5 Manual Review vs. AG

The second approach for deriving detection statistics compared the *Zc* groups produced by the AG with *Zc* groups found during the same time periods by manual analysis using MMAMMAL. In generating the detection statistics, the *Zc* groups found manually were considered the 'truth.' Correction factors, derived from the detection statistics, were applied to the AG group dive start results to find the 'true' number of *Zc* group dive starts present.

One hundred random 1-hour samples were identified between 2010 and 2015, and 31 of these random samples were manually reviewed for the presence of *Zc*. *Zc* group dive starts, i.e., group dives that began within the one hour sample period, were used for the analysis. The CS-SVM algorithm output, which better discriminates *Zc* from delphinids, was used for the analysis. As CS-SVM only runs on the newer hydrophones ( $\geq 100$ ), only these hydrophones were included in the analysis. However, as *Zc* detections sometimes appear more clearly on the legacy hydrophones (1 – 88) when reviewing the archives in MMAMMAL, they were used as cues to help determine if the clicks on the nearby newer hydrophones were from *Zc* or delphinids.

*Zc* can be identified in MMAMMAL by appearance of the pattern of clicks (figure 8), which have an ICI of about 0.5 seconds, and bandwidth extending to 48 kHz, and varying between about 12 and 24 kHz on the lower end of the band. As the animals scan their heads, neighboring hydrophones are ensonified, with most of the clicks on one or two 'center' hydrophones. The vocal period lasts for roughly 30 – 40 minutes.

A two-step process was used to identify the *Zc* group dive starts. First, the range was divided into quarters (north, south, east, and west), with 22 or 23 hydrophones per quarter. All hydrophones in a quarter were manually reviewed by playing back the archive files through

MMAMMAL and identifying any hydrophones that potentially had *Zc* clicks. The start times of the *Zc* click-trains were noted, and a confidence level of 1 or 2 was assigned. A '1' represented a high confidence the clicks were from *Zc*, and '2' a possibility the clicks may either be delphinid (in particular Risso's dolphin), or a combination of *Zc* and delphinid. *Zc* usually can be clearly identified, but there are times when it is not obvious. Figure 8 shows the difference between (a) high confidence *Zc* clicks; (b) lower confidence *Zc* clicks, which are either *Zc* with dolphins, or possibly just dolphins; and (c) clicks which are clearly delphinid.

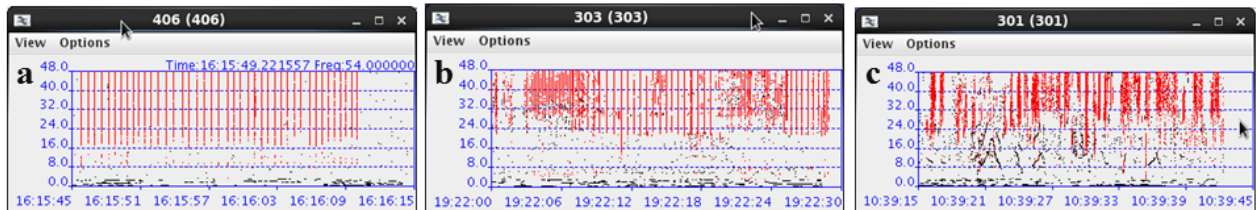


Figure 7. Rating of Clicks: A) Confidence = 1 *Zc* Clicks, B) Confidence = 2 *Zc* Clicks, C) Delphinid Clicks

After all hydrophones were reviewed, those identified in the first pass as potentially *Zc* were plotted on a map of the range, and evaluated again to determine which clicks constituted a *Zc* group, based on the temporal and spatial overlap of the click-trains. A group typically would include hydrophones within a baseline of the hydrophone which recorded the highest click density (called the center hydrophone), and with a group vocal period of less than one hour. At times neighboring groups ensoufy some common hydrophones. The *Zc* groups that were formed contained exclusively or mostly high confidence *Zc* clicks. At the conclusion of the second pass the number of dive starts, along with start and stop times of the hydrophones belonging to each group's dive start, were recorded for each of the samples. These results were then compared to the automated results produced by the AG programs. At times the manual groups were adjusted if it was determined that a group was not correctly classified manually.

The total number of manual group dive starts and total number of AG dive starts were first annotated for each sample. Then, for each sample, the groups were placed into one of four categories: a) exact matches, b) confused matches, c) manual only (false negatives, FN), or d) auto-grouper only (false positives, FP). A group was considered an exact match if: 1) the groups had at least one hydrophone in common, 2) the hydrophones were not part of another group, and 3) the time periods overlapped. The confused matches occurred when all or some of the same hydrophones were identified by both the manual process and the AG program, and the time periods overlapped, but the number of groups and/or the hydrophone combinations forming the groups were not the same. For the confused matches, both the total number of manual groups and the total number of AG groups were noted. The manual-only cases consisted of groups only identified manually (FN), and the AG-only cases were those identified solely by the AG (FP).

Prior to calculating the detection statistics from these data, the dive starts under the confused matches category were reassigned to either the exact matches, FN, or FP category with the following procedure (Table 5):

1. The minimum number of either the manual dive starts or AG dive starts for the confused matches was calculated and added to the exact matches for each sample. This sum was listed under the heading 'Correctly Detected.'
2. Under the confused matches category, if there were more manual dive starts than AG dive starts, then the difference was added to the FNs; otherwise the difference was added to the FPs. This was equivalent to calculating the new FN as the total number of manual dive starts minus the number correctly detected, and the new FP as the total number of AG dive starts minus the number correctly detected.

*Table 5. Corrected Comparison of Filtered AGI Output, all Hydrophones, with Manual Dive Starts*

<b>AutoGrouper #1 - filtered, all hyds</b>									
Sample #	Total # Manual Dive Starts	Total # AG Dive Starts	# Exact Matches	# Confused Matches		Min of Confused	Correctly Detected	# Dive Starts Manual Only (FN)	# Dive Starts AG Only (FP)
				# Manual Dive Starts	# AG Dive Starts				
45	2	2	2	0	0	0	2	0	0
46	0	0	0	0	0	0	0	0	0
47	7	7	4	3	3	3	7	0	0
49	9	7	7	0	0	0	7	2	0
50	3	7	3	0	0	0	3	0	4
51	5	5	4	0	0	0	4	1	1
53	3	3	1	2	2	2	3	0	0
56	2	1	1	0	0	0	1	1	0
58	1	1	1	0	0	0	1	0	0
59	1	1	1	0	0	0	1	0	0
61	0	0	0	0	0	0	0	0	0
62	0	0	0	0	0	0	0	0	0
65	0	0	0	0	0	0	0	0	0
66	1	1	1	0	0	0	1	0	0
68	2	1	1	0	0	0	1	1	0
71	1	1	1	0	0	0	1	0	0
73	2	1	1	0	0	0	1	1	0
75	4	3	3	0	0	0	3	1	0
76	7	4	4	0	0	0	4	3	0
78	2	3	0	2	1	1	1	1	2
81	1	0	0	0	0	0	0	1	0

84	2	1	1	0	0	0	1	1	0
87	5	6	4	1	2	1	5	0	1
90	4	4	3	0	0	0	3	1	1
92	6	5	2	4	3	3	5	1	0
93	5	5	0	4	3	3	3	2	2
95	1	0	0	0	0	0	0	1	0
96	1	0	0	0	0	0	0	1	0
97	3	2	2	0	0	0	2	1	0
99	2	3	2	0	0	0	2	0	1
100	2	1	0	0	0	0	0	2	1
	<b>84</b>	<b>75</b>	<b>49</b>	<b>16</b>	<b>14</b>	<b>13</b>	<b>62</b>	<b>22</b>	<b>13</b>

The detection statistics were then calculated, along with correction factors to apply to the number of AG groups detected in order to derive the ‘true’ number of *Zc* group dive starts present. The PD was calculated as the sum over all samples of the dive starts correctly detected divided by the sum over all samples of the number of manual dive starts. The percentage of false negatives (dive starts missed by the AG) was the sum over all samples of the FN divided by the sum over all samples of the number of manual dive starts; and the percentage of false positives (dive starts misidentified by the AG) was the sum over all samples of the FP divided by the sum over all samples of the number of AG dive starts. Table 6 shows the resulting detection statistics for the dive start data in Table 5.

*Table 6. Detection Statistics for Dive Start Data.*

<b>PD</b>	0.738
<b>FN</b>	0.262
<b>FP</b>	0.173

FP and FN correction factors for the AG dive start results were then derived as follows:

1. The FP correction factor =  $1 - (\text{sum over all samples of FP} / \text{sum over all samples of the AG dive starts})$
2. The FN correction factor =  $1 + (\text{sum over all samples of FN} / (\text{sum over all samples of the AG dive starts} * \text{FP correction factor}))$ .

These steps essentially begin with the number of AG dive starts, subtract the number of FP and add the number of FN to recover the number of manual dive starts, which are considered the ‘true’ number of *Zc* dive starts. Note in Table 7 that after applying the correction factors to the number of AG dive starts in Table 5 (75) the number of manual dive starts in Table 5 (84) is recovered.

*Table 7. Correction Factors for the AG Dive Start Results.*

		# Corrected AG Dive Starts
<b>FP Correction Factor</b>	0.827	62
<b>FN Correction Factor</b>	1.355	84

The detection statistics were considered for two cases: for all group dive starts within the sample hour, and for all group dive starts within the sample hour except 'edge-only' cases. The 'edge-only' cases are those groups that only contain hydrophones on the edge of the range. These are removed as it is likely that the associated group occurs outside the range boundary. If either the AG or the manual analysis reported an 'edge-only' group, both this group and its matching group in the alternate method were removed from the analysis. The detection statistics and correction factors for both the 'all hydrophone' and 'no edge-only' cases are shown in Tables 8 and 9, respectively.

*Table 8. Auto-grouper detection statistics for the case including all hydrophones, and for the case removing 'edge-only' hydrophones.*

<b>Zc Dive Starts</b>				
<b>Algorithm</b>	<b>n</b>	<b>PD</b>	<b>% FN</b>	<b>% FP</b>
Autogrouper - filtered, all hyds	31	0.738	0.262	0.173
Autogrouper - filtered, no edge only	31	0.759	0.241	0.185

*Table 9. Correction factors for the case including all hydrophones, and for the case removing 'edge-only' hydrophones.*

<b>Algorithm</b>	<b>Correction Factors</b>	
	<b>FP</b>	<b>FN</b>
Autogrouper - filtered, all hyds	0.827	1.355
Autogrouper - filtered, no edge only	0.815	1.318

## 6. Long Term Abundance and Density

### 6.1 Background

Expert observers have identified *Md* at AUTEK and PMRF and *Zc* at AUTEK and SOAR [14, 15, 16]. Beaked whales associate and dive together in groups. They execute deep foraging dives

at measurable rates and echolocate only during these dives [11, 17]. Therefore, the detection of beaked whale echolocation clicks indicates a group of animals in a deep foraging dive. If the mean group size and foraging dive rate are known, animal abundance and density can be estimated [1, 18].

M3R provides long-term monitoring of beaked whales on all three major ranges using the dive counting method developed for *Md* at AUTECH. Tracking trends in abundance over months, seasons, and years is possible as data become available. Over time, M3R passive acoustic recordings will provide a more robust, long-term beaked whale abundance estimate. Such estimates can be cross-validated with those produced using photo-ID data via mark-recapture methods [15].

The dive counting method requires an estimate of group size and dive rate. *Zc* group size in SOCAL was derived from visual sighting data from collaborating on-water partners. Dive rate was measured via depth recording satellite tags [13, 19, 20].

## 6.2 Dive Counting Methodology

The dive counting method as given below was applied to estimate the overall abundance ( $N$ ) at both SOAR and PMRF [1].

$$N = \frac{n_d s}{r_d T} \quad \begin{array}{l} n_d = \text{total number of dive starts} \\ s = \text{average group size} \\ r_d = \text{dive rate (dives/unit time)} \\ T = \text{time period over which the measurement was made} \end{array} \quad (3)$$

Where density ( $D$ ) is given by

$$D = \frac{N}{A} \quad A = \text{measurement Area} \quad (4)$$

The method requires the detection of beaked whale clicks that are then used to detect the presence of GVPs. Visual data are used to estimate the mean number of animals per group [15, 19]. The rate of deep foraging dives is derived from satellite tag data [19]. For density estimation the detection range was derived from measurements for *Md* at AUTECH [16, 1].

## 6.3 SOAR Abundance

The dive-counting passive acoustic method described above was applied to SOAR detection archives from 2010 to 2014. The SOAR archives include detection reports from the Jarvis CS-SVM classifiers. The CS-SVM provides improved discrimination between *Zc* and dolphin echolocation clicks, with a per

click correct classification rate of greater than 90%. This is particularly important at SOAR where the abundance of interfering species' calls is particularly high.

Click trains were first compiled for CS-SVM *Zc* click detection reports. The click trains were then associated into groups using the auto-grouper software. The start and stop time of uninterrupted data periods within the archives were determined. A new period was marked if no group was detected for a period of 24 hours. It should be noted that the M3R processor was disabled for some operations which led to data gaps.

Our abundance estimates showed no decline in population over a five-year period. Data originally analyzed in 2015, filtered to remove edge-only hydrophones, were corrected based on the detection statistics as described above. The results are shown in Figures 9 and 10 below.

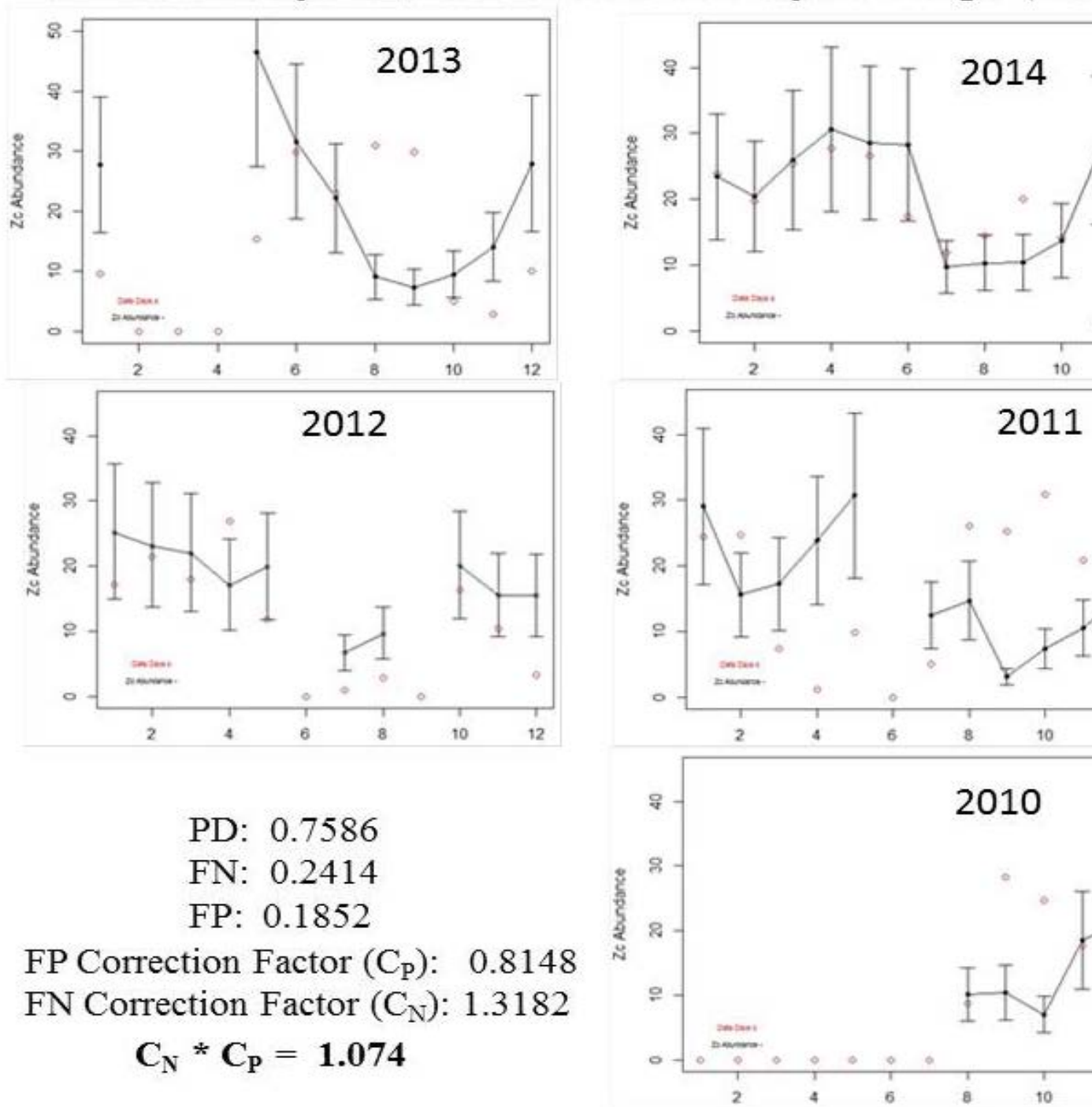


Figure 8. Yearly abundance at SOAR corrected for the estimated false alarm rate and probability of detection. The data are plotted as month on the x-axis and total number of animals on the y-axis.

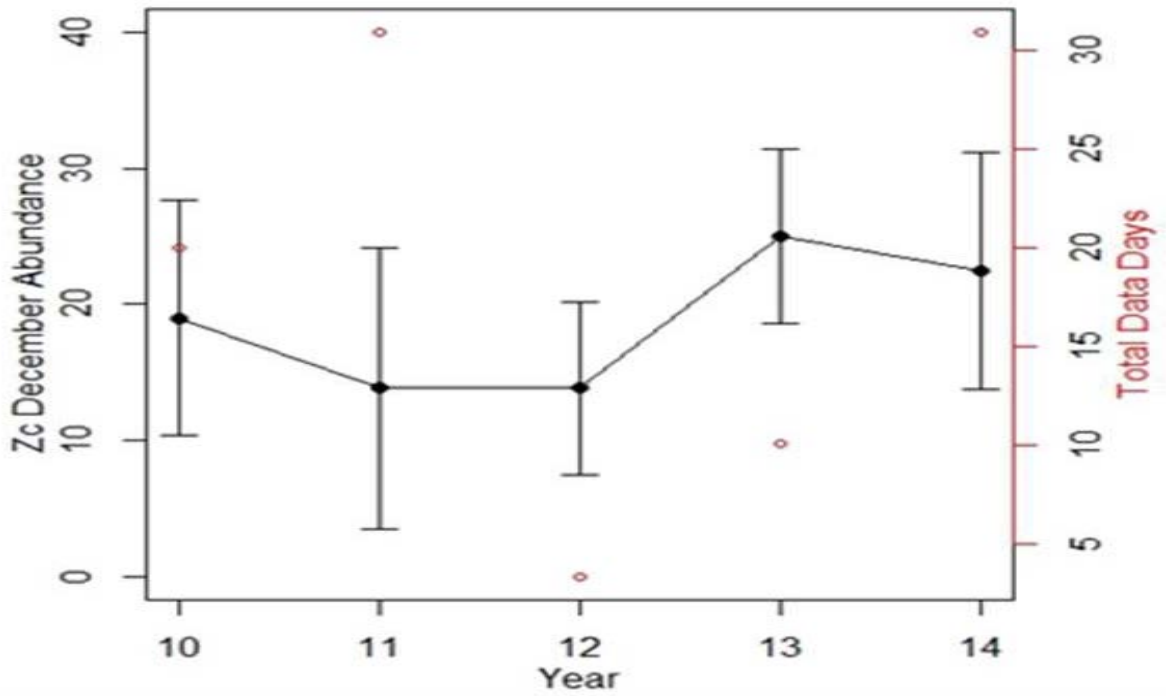


Figure 9. Corrected estimate of yearly abundance at SOAR for the month of December from 2010 to 2014.

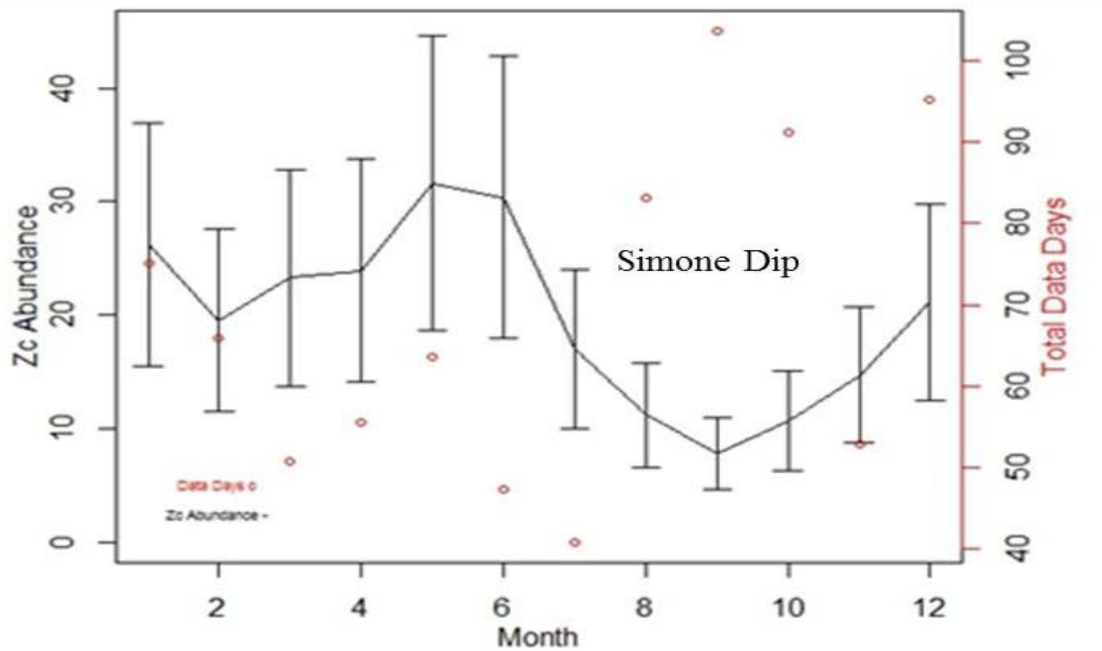


Figure 10. Corrected composite estimate of monthly abundance at SOAR with combined 2010-2014 data. Note: the abundance depression that reaches a minimum in September was first

reported by Simone Baumann-Pickering (the “Simone Dip”)

### 6.3 PMRF Abundance

Initial abundance values were also derived for PMRF. Five years of data archives, from 2010 to 2014, were examined.

To parameterize the abundance equation, the mean dive rate and group size from Baird *et al.*, 2008 were used (Table 8) [21].

Table 10. Mean dive rate and group size estimates

Mean Dive Rate (dive/hr.)	Var	Dives/Day	Mean Group Size	Var
0.46	0.01	11.04	3.69	5.71

An initial abundance estimate for a limited 85 hour period in 2010, previously completed with data extracted manually by an analyst, suggested on the order of a dozen *Md* in three groups on the range at a time (Table 9).

Table 11. 2010 estimate of *Md* abundance and number of groups present on PMRF, with groups manually identified over an 85.15 hour period

Animals	Groups
12.34 (6.63-18.055)	3.34 (1.8-4.89)

In FY 16 data from all M3R tests conducted from 2010-2014 on the PMRF range were analyzed.

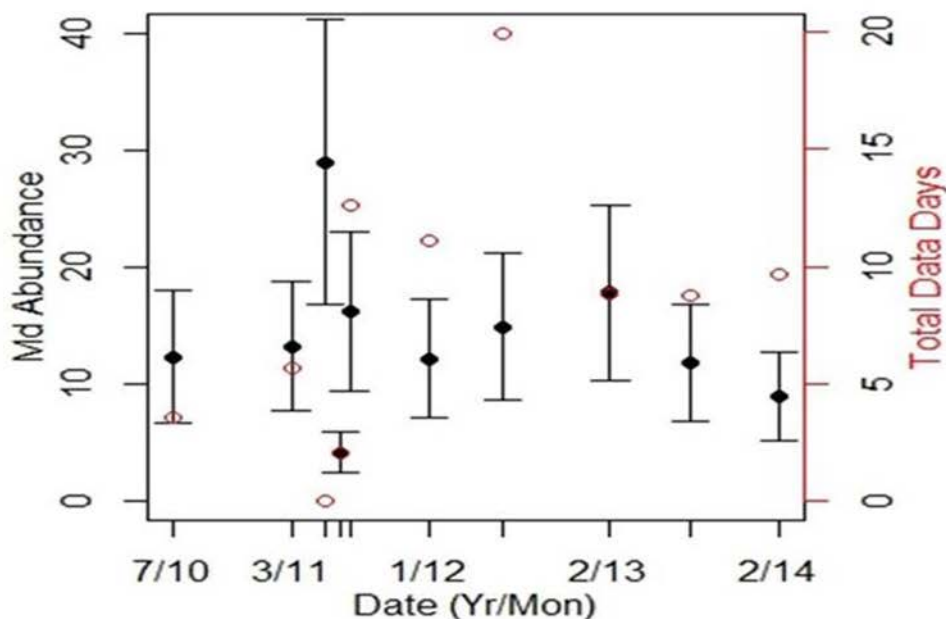


Figure 11. Abundance estimates for 2010 - 2014

#### 6.4 Comparison of M3R and SPAWAR Algorithms

To compare *Md* detections for PMRF between SPAWAR and NUWC, data from 2011 – 2014 were examined to identify periods that were concurrently recorded by both organizations. Four time periods were selected that ranged from just over one day (28.4 hours) to over four days (110.7 hours).

An initial data comparison was conducted. NUWC first extracted click trains from detection archives. These were input into M3R Auto-Grouper software to isolate *Md* groups. These data were then provided to SPAWAR, who compared the output of their algorithms to NUWC's. Automated *Md* group detections were compared to determine how many dives were detected by both algorithms and how many were only detected by only one. More work is required to complete the comparison, but initial results are shown in Tables 10 and 11. Preliminary results show a good agreement between SPAWAR and NUWC, with a PD varying between 0.67 and 0.85, and *Md* density ranging from 0.018 to 0.037.

At AUTEK and SOAR the probability of detection by NUWC algorithms was found to be 75-80% and correction factors for false positives and false negatives were derived. Similarly, it is essential to derive correction factors for PMRF, a process which is underway.

Table 12. A comparison of PMRF Md dive detections between SPAWAR and NUWC.

	Mar-11		Jul-11		Jan-12		Feb-14	
	all phones	southern phones						
SPAWAR raw dets	63		79		171		178	
SPAWAR validated dets	46	32	66	34	143	102	160	130
SPAWAR/NUWC matches	35	22	51	26	115	78	98	81
NUWC unmatched	24	16	16	12	52	42	26	23
NUWC Dets total	59	38	69	38	167	120	124	104
Total dives detected	70	48	82	46	195	144	186	153
SPAWAR missed	1	0	0	0	3	1	5	3
SPAWAR false positive	17		13		28	0	18	
NUWC missed	11	10	15	8	28	24	62	49
NUWC false positive	0	0	0	0	2	2	10	10

Table 13. PMRF Md density calculations using SPAWAR data, NUWC data, and combined data.

	Mar 2011			Jul 2011			Jan 2012			Feb 2014		
	combined	SPAWAR	NUWC									
n (#dives)	48	32	38	46	34	38	195	102	120	153	130	104
s (mean group size)	3.6	3.6	3.6	3.6	3.6	3.6	3.6	3.6	3.6	3.6	3.6	3.6
r (dive time)	0.43	0.43	0.43	0.43	0.43	0.43	0.43	0.43	0.43	0.43	0.43	0.43
T (time)	33.1	33.1	33.1	28.4	28.4	28.4	99.9	99.9	99.9	110.7	110.7	110.7
A (area)	440	440	440	440	440	440	440	440	440	440	440	440
c = 0	0	0	0	0	0	0	0	0	0	0	0	0
c (prob false positives)	0	0	0	0	0	0	0	0.00	0.02	0	0	0.10
p = 1	1	1	1	1	1	1	1	1	1	1	1	1
p (prob detection)	1	0.67	0.79	1	0.74	0.83	1	0.71	0.83	1	0.85	0.68
D=(1-c)*n*s/P*r*T*A	<b>0.028</b>	<b>0.018</b>	<b>0.022</b>	<b>0.031</b>	<b>0.023</b>	<b>0.025</b>	<b>0.037</b>	<b>0.019</b>	<b>0.023</b>	<b>0.026</b>	<b>0.022</b>	<b>0.018</b>
	<b>0.028</b>	<b>0.028</b>	<b>0.028</b>	<b>0.031</b>	<b>0.031</b>	<b>0.031</b>	<b>0.037</b>	<b>0.027</b>	<b>0.027</b>	<b>0.026</b>	<b>0.026</b>	<b>0.024</b>

The completion of this analysis will enable the expanded joint analysis of both past and future archives in an effort to provide an abundance estimate over multiple years with a measure of uncertainty. An example of the use of combined data analysis is provided above in Table 11.

## Works Cited

- [1] D. Moretti, T. Marques, L. Thomas, N. DiMarzio, A. Dilley, R. Morrissey, E. McCarthy, J. Ward and S. Jarvis, "A dive counting density estimation method for Blainville's beaked whale (*Mesoplodon densirostris*) using a bottom-mounted hydrophone field as applied to a Mid-Frequency Active (MFA) sonar operation," *J. Applied Acoustics*, vol. 71, no. 11, pp. 1036-1042, 2010.
- [2] N. A. DiMarzio and S. M. Jarvis, *Temporal and Spatial Distribution and Habitat Use of Cuvier's Beaked Whales on the U.S. Navy's Southern California Anti-submarine Warfare Range (SOAR): Data Preparation*. TM 16-090. Newport, RI: Naval Undersea Warfare Center (NUWC), 2016.
- [3] S. M. Jarvis, R. P. Morrissey, D. J. Moretti, N. A. DiMarzio and J. A. Shaffer, "Marine Mammal Monitoring on Navy Ranges (M3R): A toolset for Detection, Localization, and Monitoring of marine mammals in open ocean environments," *Marine Technology Society Journal*, vol. 48, no. 1, pp. 5-20, 2014.
- [4] D. Moretti, N. DiMarzio, R. Morrissey, J. Ward and S. Jarvis, "Open ocean marine mammal monitoring using widely spaced bottom mounted hydrophones," *U.S. Navy Journal of Underwater Acoustics*, vol. 52, pp. 651-668, 2002.
- [5] S.W. Martin, C. R. Martin and B. Matsuyama, "Opportunistic behavioral-response studies of baleen whales in response to US Navy sonar training off Kauai, Hawaii," *Journal of the Acoustical Society of America*, vol. 140, no. 4, p. 3413, 2016.
- [6] E. McCarthy, D. Moretti, L. Thomas, N. DiMarzio, A. Dilley, R. Morrissey, J. Ward, A. Izzi and S. Jarvis, "Changes in spatial and temporal distribution and vocal behavior of Blainville's beaked whales (*Mesoplodon densirostris*) during multiship exercises with mid-frequency sonar," *Marine Mammal Science*, vol. 27, no. 3, pp. E206-E226, 2011.
- [7] S. L. DeRuiter, B. L. Southall, J. Calambokidis, W. M. X. Zimmer, D. Sadykova, E. A. Falcone, A. S. Friedlaender, J. E. Joseph, D. Moretti, G. S. Schorr, L. Thomas and P. L. Tyack, "First direct measurements of behavioural response by Cuvier's beaked whales to mid-frequency active sonar," *Biology Letters*, vol. 9, no. 4, 20130223. doi: 10.1098/rsbl.2013.0223, 2013.
- [8] P. L. Tyack, W. M. X. Zimmer, D. Moretti, B. L. Southall, D. E. Claridge, J. W. Durban, C. W. Clark, A. D'Amico, N. DiMarzio, S. Jarvis, E. McCarthy, R. Morrissey, J. Ward and I. L. Boyd, "Beaked whales respond to simulated and actual Navy sonar," *PLoS ONE*, vol. 6, e17009. doi:17010.11371/journal.pone.0017009, 2011.
- [9] D. Moretti, L. Thomas, T. Marques, J. Harwood, A. Dilley, B. Neales, J. Shaffer, E. McCarthy, L. New, S. Jarvis and R. Morrissey, "A risk function for Blainville's beaked whales (*Mesoplodon densirostris*) derived from mid-frequency active sonar," *PLoS ONE*, vol. 9, e85064. doi:85010.81371/journal.pone.0085064, 2014.
- [10] L. F. New, D. J. Moretti, S. K. Hooker, and S. E. Simmons, "Using energetic models to investigate the survival and reproduction of beaked whales (family Ziphiidae)," *PLoS ONE*, vol. 8, e68725. doi:68710.61371/journal.pone.006872, 2013.
- [11] M. Johnson, P. T. Madsen, W. M. X. Zimmer, N. Aguilar de Soto and P. L. Tyack, "Beaked whales echolocate on prey," *Proceedings of the Royal Society of London, Part B*, vol. 271, pp. S383-S386, 2004.

- [12] J. W. Shaffer, D. Moretti, S. Jarvis, P. Tyack and M. Johnson, "Effective beam pattern of the Blainville's beaked whale (*Mesoplodon densirostris*) and implications for passive acoustic monitoring," *Journal of the Acoustical Society of America*, vol. 133, no. 3, pp. 1770-1784, 2013.
- [13] G. S. Schorr, E. A. Falcone, D. J. Moretti and R. D. Andrews, "First long-term behavioral records from Cuvier's beaked whales (*Ziphius cavirostris*) reveal record-breaking dives," *PLoS ONE*, vol. 9, e92633. doi:92610.91371/journal.pone.0092633, 2014.
- [14] W. M. X. Zimmer, J. Harwood, P. L. Tyack, M. P. Johnson and P. T. Madsen, "Passive acoustic detection of deep-diving beaked whales," *Journal of the Acoustical Society of America*, vol. 124, no. 5, pp. 2823-2832, 2008.
- [15] E. A. Falcone, G. S. Schorr, A. B. Douglas, J. Calambokidis, E. Henderson, M. F. McKenna, J. Hildebrand and D. Moretti, "Sighting characteristics and photo-identification of Cuvier's beaked whales (*Ziphius cavirostris*) near San Clemente Island, California: A key area for beaked whales and the military?," *Marine Biology*, vol. 156, pp. 2631-2640, 2009.
- [16] D. E. Claridge, "Population ecology of Blainville's beaked whales (*Mesoplodon densirostris*)," PhD Thesis, University of St Andrews. 2013.
- [17] M. Johnson, P. T. Madsen, W. M. Zimmer, N. Aguilar de Soto and P. L. Tyack, "Foraging Blainville's beaked whales (*Mesoplodon densirostris*) produce distinct click types matched to different phases of echolocation," *Journal of Experimental Biology*, vol. 209, pp. 5038-5050, 2006.
- [18] T. A. Marques, L. Thomas, S. W. Martin, D. K. Mellinger, J. A. Ward, D. J. Moretti, D. Harris and P. L. Tyack, "Estimating animal population density using passive acoustics," *Biological Reviews of the Cambridge Philosophical Society*, vol. 88, pp. 287-309, 2013.
- [19] R. W. Baird, G. S. Schorr, D. L. Webster, S. D. Mahaffy, D. J. McSweeney, M. B. Hanson and R. D. Andrews, "Open-ocean movements of a satellite-tagged Blainville's beaked whale (*Mesoplodon densirostris*): Evidence for an offshore population in Hawai'i?," *Aquatic Mammals*, vol. 37, pp. 506-511, 2011.
- [20] R. W. Baird, G. S. Schorr, D. L. Webster, D. J. McSweeney, M. B. Hanson and R. D. Andrews, "Movements and habitat use of satellite-tagged false killer whales around the main Hawaiian Islands.," *Endangered Species Research*, vol. 10, pp. 107-121, 2010.
- [21] R. W. Baird, D. L. Webster, G. S. Schorr, D. J. McSweeney and J. Barlow, "Diel variation in beaked whale diving behavior.," *Marine Mammal Science*, vol. 24, pp. 630-642, 2008.